Macroscopic Axisymmetric Lattice Boltzmann Method (MacAxLAB)

Jian Guo Zhou

Department of Computing and Mathematics
Manchester Metropolitan University
Manchester, M1 5GD, UK
J.Zhou@mmu.ac.uk

Abstract

The author has recently proposed a macroscopic lattice Boltzmann method (MacLAB) for the Navier-Stokes equations. The method is formulated for the first time to retain the streaming step but remove the collision step in the two integral steps of the standard lattice Boltzmann method. It relies on one fundamental parameter of lattice size δx in the model. This leads to a revolutionary and precise minimal "Lattice" Boltzmann method, which directly uses physical variables as boundary conditions with less required storage for more accurate and efficient simulations. In this paper, the MacLAB is further developed for solving incompressible axisymmetric flow equations (MacAxLAB). The model is validated through simulations of a 3D unsteady Womersley flow and two 3D steady cylindrical cavity flows. The numerical results have compared with other numerical ones and available analytical solutions; it shows that the MacAxLAB is applicable and accurate for modelling incompressible axisymmetric flow.

Keywords: Macroscopic lattice Boltzmann method, axisymmetric flow, computational fluid dynamics, numerical method.

1. Introduction

The lattice Boltzmann method (LBM) is proposed as a simple model for fluid flows. It is a highly simplified model using a finite number of particles. Since then, it has been developed into a very efficient and flexible alternative numerical method in computational fluid dynamics. The method has been extended to solve many other flow problems. For example, Swift et al.

applied the lattice Boltzmann method to simulate nonideal fluids [1]. Spaid and Phelan, Jr. solved the Brinkman equation using the LBM [2]. Zhou developed the LBMs for shallow water flows [3] and groundwater flows [4].

The axisymmetric flow case encompasses numerous important flow problems in practice [5–9]. Halliday et al. [10] firstly studied the LBM for axisymmetric flows in 2001 through introduction of two source terms into the lattice Boltzmann equation. His method has successfully been applied to a number of axisymmetric flow problems [5, 6, 11]. After realising that the one term in the momentum equation related to radial velocity is missing from the formulation of Halliday et al., which causes large errors for axisymmetric flows with significant radial velocities in non-straight pipes, Lee et al. [12] corrected it and obtained an accurate solution to flows when radial velocities cannot be ignored. In addition, the method of Halliday et al. has been extended to multiphase flow by Premnath and Abrahamand [7] and two phase flow with large density ratio by Shiladitya and Abraham [9]. Following the similar idea to Halliday et al., Reis and Phillips [8, 13] modified the source terms in a slightly different manner without the mistake made by Halliday et al. The main drawbacks of these methods are that the second source term involves more complicated terms than the original equations and the added forces cause inconsistency in the dimension of the lattice Boltzmann equation.

In 2009, Guo et al. [14] proposed an axisymmetric lattice Boltzmann model from the continuous Boltzmann equation in cylindrical coordinates for axisymmetric flows with or without swirling in the framework of the lattice Boltzmann approach. Furthermore, Li et al. presented an improved axisymmetric lattice Boltzmann scheme including rotational effect [15]. Both models of Guo et al. and Li et al. are suitable for general axisymmetric rotational flows and the added source or force terms to the schemes contains no velocity gradient, which are simpler and easier to use compared to other existing methods. However, these two methods share the same weaknesses: (a) the source or force terms contains more terms than those in the original governing equations; (b) the expressions for calculating the macroscopic variables like velocities take complex forms instead of the conventional simple sum of the distribution functions due to elimination of the implicitness in the schemes, complicating the algorithm; and (c) each gives its own expression for the viscosity that is different from the standard definition in the lattice Boltzmann dynamics. In addition, Zhou developed an axisymmetric lattice Boltzmann method without swirling [16]. The method has many features close to the standard lattice Boltzmann approach to the Navier-Stokes equations, e.g., simple procedure, good numerical stability and standard calculations for macroscopic parameters like velocity, which have been confirmed in the research by Huang and Lu [17], Li et al. [18], and Tang. et al. [19]. Its only disadvantage is that the introduced force term contains velocity gradients. Later, Zhou [20] improved this method and developed the AxLAB® to overcome the aforementioned weaknesses for generic axisymmetric flows involving swirling. Its main features are that the method contains no velocity gradient and retains all the original desired advantages: (a) the source terms are the same as the ones additional to the Navier-Stokes equations and (b) the standard calculations for density and velocities are preserved as those in the conventional LBM. The main weakness of all these existing methods is that the physical variables such as velocity and density cannot be used as boundary conditions without being converted to the corresponding distribution functions. Also, the no slip boundary condition cannot be exactly achieved through application of the most popular and efficient bounce-back scheme. These drawbacks have been removed by Zhou [21] in his newly developed macroscopic lattice Boltzmann method (MacLAB) for Navier-Stokes equations for fluid flows. In this paper, the MacLAB is extended to solve the axisymmetric flow equations.

2. Axisymmetric Flow Equations

The governing equations for the incompressible axisymmetric flows are continuity and momentum equations. They can be written in a cylindrical coordinate system as [22]

$$\frac{\partial u_j}{\partial x_j} = -\frac{u_r}{r} \tag{1}$$

and

$$\begin{aligned}\frac{\partial u_i}{\partial t} &+ \frac{\partial (u_i u_j)}{\partial x_j} = -\frac{1}{\rho}\frac{\partial p}{\partial x_i} + \nu \frac{\partial}{\partial x_j}\left(\frac{\partial u_i}{\partial x_j} + \frac{\partial u_j}{\partial x_i}\right) \\ &+ \frac{\nu}{r}\left(\frac{\partial u_i}{\partial r} + \frac{\partial u_r}{\partial x_i}\right) - \frac{u_i u_r}{r} - \frac{2\nu u_i}{r^2}\delta_{ir},\end{aligned} \tag{2}$$

where ρ is the density; p is the pressure; t is the time; ν is the kinematic viscosity; i is the index standing for r or x; r and x are the coordinates in radial and axial directions, respectively; u_i is the component of velocity in i direction; δ_{ij} is the Kronecker delta function defined by

$$\delta_{ij} = \begin{cases} 0, & i \neq j, \\ 1, & i = j; \end{cases} \tag{3}$$

and the repeated indexes are the Einstein summation convention, which means a summation over the space coordinates. Such a convention is used throughout the paper without further indication.

3. Macroscopic Lattice Boltzmann Method

3.1. Lattice Boltzmann equation

Zhou's reformulated lattice Boltzmann equation with source or sink and force terms for axisymmetric flows, AxLAB®, reads [20]:

$$\begin{aligned} f_\alpha(\mathbf{x} + \mathbf{e}_\alpha \delta t, t + \delta t) &= f_\alpha(\mathbf{x}, t) - \frac{1}{\tau}(f_\alpha - f_\alpha^{eq}) \\ &\quad - Z_r \left[\frac{(2\tau - 1) e_{\alpha r} \delta t}{2\tau r} \right] (f_\alpha - f_\alpha^{eq}) \\ &\quad + w_\alpha \theta \delta t + 3 w_\alpha \frac{\delta t}{e^2} e_{\alpha i} F_i, \end{aligned} \tag{4}$$

where f_α is the distribution function of particles; f_α^{eq} is the local equilibrium distribution function; δt is the time step; $\mathbf{x}$ is the space vector i.e., $\mathbf{x} = (r, x)$; $e = \delta x / \delta t$; δx is the lattice size; Z_r is a constant taking value of 0 for $r = 0$ or 1 for $r \neq 0$; w_α is the weight given by Eq. (7); θ is the source or sink term,

$$\theta = -\frac{\rho u_r}{r}; \tag{5}$$

F_i is the force term defined by

$$F_i = -\frac{\rho u_i u_r}{r} - \frac{2\rho\nu u_i}{r^2} \delta_{ir}; \tag{6}$$

$e_{\alpha i}$ is the component of $\mathbf{e}_\alpha$, which is the velocity vector of a particle in the α link. It can be seen from the recovery in Appendix A that the term related to $1/r$ in the above equation (4) recovers the second term, Λ_{ir}/r, on the right-hand side of Eq. (A.12) that is zero according to L'Hôpital's rule when $r = 0$ and hence it does not exist at $r = 0$ [7, 23].

If the nine-velocity square lattice (D2Q9) shown in Fig. 1 is used, w_α is defined as

$$w_\alpha = \begin{cases} \frac{4}{9}, & \alpha = 0, \\ \frac{1}{9}, & \alpha = 1,\ 3,\ 5,\ 7, \\ \frac{1}{36}, & \alpha = 2,\ 4,\ 6,\ 8; \end{cases} \tag{7}$$

and $\mathbf{e}_\alpha$ is

$$\mathbf{e}_\alpha = \begin{cases} (0,0), & \alpha = 0, \\ \lambda_\alpha e \left[\cos\frac{(\alpha-1)\pi}{4}, \sin\frac{(\alpha-1)\pi}{4}\right], & \alpha \neq 0, \end{cases} \tag{8}$$

with λ_α,

$$\lambda_\alpha = \begin{cases} 1, & \alpha = 1,\ 3,\ 5,\ 7, \\ \sqrt{2}, & \alpha = 2,\ 4,\ 6,\ 8. \end{cases} \tag{9}$$

The fluid density ρ and velocity u_i are determined from the distribution

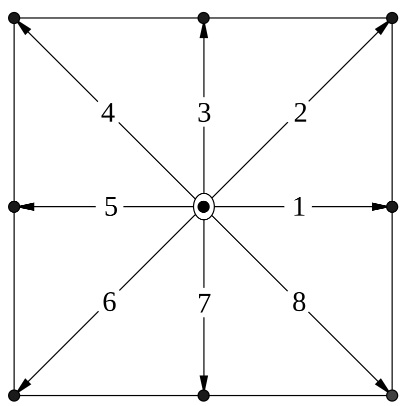

Figure 1: Nine-velocity square lattice (D2Q9).

function in the same manner as that in the standard LBM for the Navier-Stokes equations,

$$\rho = \sum_\alpha f_\alpha, \qquad u_i = \frac{1}{\rho}\sum_\alpha e_{\alpha i} f_\alpha. \tag{10}$$

The local equilibrium distribution function f_α^{eq} is

$$f_\alpha^{eq} = w_\alpha \rho \left(1 + 3\frac{e_{\alpha i}u_i}{e^2} + \frac{9}{2}\frac{e_{\alpha i}e_{\alpha j}u_i u_j}{e^4} - \frac{3}{2}\frac{u_j u_j}{e^2}\right), \tag{11}$$

which can be shown to have the following properties,

$$\rho=\sum_{\alpha} f_{\alpha}^{eq}, \qquad u_i=\frac{1}{\rho}\sum_{\alpha} e_{\alpha i} f_{\alpha}^{eq}. \tag{12}$$

To avoid determining the density and velocity through Eq. (10) using distribution functions, Eq. (4) is rewritten as

$$\begin{aligned} f_{\alpha}(\mathbf{x},t) &= f_{\alpha}(\mathbf{x}-\mathbf{e}_{\alpha}\delta t, t-\delta t)-\frac{1}{\tau}[f_{\alpha}(\mathbf{x}-\mathbf{e}_{\alpha}\delta t, t-\delta t) \\ &- f_{\alpha}^{eq}(\mathbf{x}-\mathbf{e}_{\alpha}\delta t, t-\delta t)] \\ &- Z_r\left[\frac{(2\tau-1)e_{\alpha r}\delta t}{2\tau r}\right][f_{\alpha}(\mathbf{x}-\mathbf{e}_{\alpha}\delta t, t-\delta t) \\ &- f_{\alpha}^{eq}(\mathbf{x}-\mathbf{e}_{\alpha}\delta t, t-\delta t)] \\ &+ w_{\alpha}\delta t\theta+3w_{\alpha}\frac{\delta t}{e^2}e_{\alpha i}F_i. \end{aligned} \tag{13}$$

After substitution of $\tau=1$ into the above equation following Zhou's idea in MacLAB [21], it can be simplified to

$$\begin{aligned} f_{\alpha}(\mathbf{x},t) &= f_{\alpha}^{eq}(\mathbf{x}-\mathbf{e}_{\alpha}\delta t, t-\delta t)-Z_r\frac{e_{\alpha r}\delta t}{2r}f_{\alpha}^{neq}(\mathbf{x}-\mathbf{e}_{\alpha}\delta t, t-\delta t) \\ &+ w_{\alpha}\delta t\theta+3w_{\alpha}\frac{\delta t}{e^2}e_{\alpha i}F_i, \end{aligned} \tag{14}$$

in which f_{α}^{neq} is the non-equilibrium distribution function,

$$f_{\alpha}^{neq}=f_{\alpha}-f_{\alpha}^{(eq)}. \tag{15}$$

Taking $\sum$ Eq. (14) and $\sum e_{\alpha i}$Eq. (14) yields

$$\begin{aligned} \sum f_{\alpha}(\mathbf{x},t) &= \sum f_{\alpha}^{eq}(\mathbf{x}-\mathbf{e}_{\alpha}\delta t, t-\delta t) \\ &- Z_r\frac{\delta t}{2r}\sum e_{\alpha r}f_{\alpha}^{(neq)}(\mathbf{x}-\mathbf{e}_{\alpha}\delta t, t-\delta t) \\ &+ \delta t\sum w_{\alpha}\theta+3\frac{\delta t}{e^2}\sum w_{\alpha}e_{\alpha i}F_i \end{aligned} \tag{16}$$

and

$$\begin{aligned} \sum e_{\alpha i}f_{\alpha}(\mathbf{x},t) &= \sum e_{\alpha i}f_{\alpha}^{eq}(\mathbf{x}-\mathbf{e}_{\alpha}\delta t, t-\delta t) \\ &- Z_r\frac{\delta t}{2r}\sum e_{\alpha r}e_{\alpha i}f_{\alpha}^{(neq)}(\mathbf{x}-\mathbf{e}_{\alpha}\delta t, t-\delta t) \\ &+ \delta t\sum w_{\alpha}e_{\alpha i}\theta+3\frac{\delta t}{e^2}\sum w_{\alpha}e_{\alpha i}e_{\alpha j}F_j. \end{aligned} \tag{17}$$

As $\sum f_\alpha(\mathbf{x},t) = \rho(\mathbf{x},t)$ and $\sum e_{\alpha i} f_\alpha(\mathbf{x},t) = \rho(\mathbf{x},t) u_i(\mathbf{x},t)$ due to the requirement for the conservation of mass and momentum in the lattice Botlzmann dynamics, we have

$$\begin{aligned}
\rho(\mathbf{x},t) &= \sum f_\alpha^{eq}(\mathbf{x}-\mathbf{e}_\alpha \delta t, t-\delta t) \\
&- Z_r \frac{\delta t}{2r} \sum e_{\alpha r} f_\alpha^{(neq)}(\mathbf{x}-\mathbf{e}_\alpha \delta t, t-\delta t) \\
&+ \delta t \sum w_\alpha \theta + 3\frac{\delta t}{e^2} \sum w_\alpha e_{\alpha i} F_i,
\end{aligned} \tag{18}$$

and

$$\begin{aligned}
\rho u_i(\mathbf{x},t) &= \sum e_{\alpha i} f_\alpha^{eq}(\mathbf{x}-\mathbf{e}_\alpha \delta t, t-\delta t) \\
&- Z_r \frac{\delta t}{2r} \sum e_{\alpha r} e_{\alpha i} f_\alpha^{(neq)}(\mathbf{x}-\mathbf{e}_\alpha \delta t, t-\delta t) \\
&+ \delta t \sum w_\alpha e_{\alpha i} \theta + 3\frac{\delta t}{e^2} \sum w_\alpha e_{\alpha i} e_{\alpha j} F_j.
\end{aligned} \tag{19}$$

According to the centred scheme [20, 24] both source term θ and force term F_i can be evaluated at the midpoint between $(\mathbf{x}-\mathbf{e}_\alpha \delta t, t-\delta t)$ and $(\mathbf{x},t)$ as

$$\theta = \theta\left(\mathbf{x} - \frac{1}{2}\mathbf{e}_\alpha \delta t, t - \frac{1}{2}\delta t\right), \tag{20}$$

and

$$F_i = F_i\left(\mathbf{x} - \frac{1}{2}\mathbf{e}_\alpha \delta t, t - \frac{1}{2}\delta t\right), \tag{21}$$

and f_α^{neq} is estimated by [25]

$$f_\alpha^{neq}(\mathbf{x},t) = -[f_\alpha^{eq}(\mathbf{x},t) - f_\alpha^{eq}(\mathbf{x}-\mathbf{e}_\alpha \delta t, t-\delta t)]. \tag{22}$$

It can be seen from Eqs. (18) - (22) that the density and velocity are determined by the macroscopic physical variables through the local equilibrium distribution function without calculating the distribution function using Eq. (4) that is required in Eq. (10) for the density and velocity. These equations form the macroscopic axisymmetric lattice Boltzmann model (MacAxLAB). It shows in Appendix A that the fluid viscosity in the absence of collision step can be naturally taken into account using the particle speed e from

$$e = 6\nu/\delta x, \tag{23}$$

instead of $e = \delta x/\delta t$ to calculate the local equilibrium distribution function f_α^{eq} from Eq. (11). Apparently, after a lattice size δx is chosen, the model is ready to simulate a flow with a viscosity ν because $(x_j - e_{\alpha j}\delta t)$ stands for a neighbouring lattice point; f_α^{eq} at time of $(t - \delta t)$ represents its known quantity at the current time; and the particle speed e is determined from Eq. (23) for use in computation of f_α^{eq}. In addition, the time step δt is no longer an independent parameter but is calculated as $\delta t = \delta x/e$, which is used in simulations of unsteady flows. Consequently, only the lattice size δx is required in the MacAxLAB for simulation of Axisymmetric flows, bringing the LBM into a precise "Lattice" Boltzmann method. This enables the model to become an automatic simulator without tuning other simulation parameters, making it possible and easy to model a large flow system when a super-fast computer such as a quantum computer becomes available in the future.

The model is unconditionally stable as it shares the same valid condition as that for f_α^{eq}, or the Mach number $M = U_c/e$ is much smaller than 1, in which U_c is a characteristic flow speed. The Mach number can also be expressed as a lattice Reynolds number of $R_{le} = U_c\delta x/\nu$ via Eq. (23). In practical simulations, it is found that the model is stable if $R_{le} = U_m\delta x/\nu < 1$ where U_m is the maximum flow speed and is used as the characteristic flow speed. The main features of the descried model are that there is no collision operator and only macroscopic physical variables such as density and velocity are required, which are directly retained as boundary conditions with a minimum memory requirement. The simulation procedure is

(a) Initialise density and velocity,
(b) Choose the lattice size δx and determine the particle speed e from Eq. (23),
(c) Calculate f_α^{eq} from Eq. (11) using density and velocity,
(d) Update the density and velocity using Eqs. (18) and (19),
(e) Apply the boundary conditions if necessary, and repeat Step (b) until a solution is reached.

The only limitation of the described model is that, for very small viscosity or high speed flow, the chosen lattice size after satisfying $R_{le} < 1$ may turn out to generate very large lattice points (Lattice points, e.g., for one dimension with length of L is calculated as $N_L = L/\delta x$ and N_L is the lattice points); if the total lattice points is too big such that the demanding computations is beyond the power of a current computer, the simulation cannot be carried out. Such difficulties may be solved or relaxed through parallel computing based on modern computer software and hardware such as GPU processors and multiple servers, and will largely or completely removed using a future super-fast computer.

3.2. Axisymmetric rotational flows

Axisymmetric rotational flows contain an azimuthal velocity u_ϕ, which is governed by the equation in a cylindrical coordinate system [22],

$$\frac{\partial u_\phi}{\partial t} + \frac{\partial (u_j u_\phi)}{\partial x_j} = \nu \frac{\partial^2 u_\phi}{\partial x_j^2} + \frac{\nu}{r}\frac{\partial u_\phi}{\partial r} - \frac{2 u_r u_\phi}{r} - \frac{\nu u_\phi}{r^2}. \tag{24}$$

Its further effect on the flow field is taken into account by adding an additional term to the force F_i in Eq. (6) as

$$F_i = -\frac{\rho u_i u_r}{r} - \frac{2\rho\nu u_i}{r^2}\delta_{ir} + \frac{\rho u_\phi^2}{r}\delta_{ir}. \tag{25}$$

Eq. (24) is an advection-diffusion equation and can be solved accurately and efficiently on a D2Q4, D2Q5 or D2Q9 lattice model [26–28]. In the present study, the D2Q9 is used and the following lattice Boltzmann equation with a source or sink term is applied,

$$\begin{aligned}\bar{f}_\alpha(\mathbf{x} + \mathbf{e}_\alpha \delta t, t + \delta t) &= \bar{f}_\alpha(\mathbf{x}, t) - \frac{1}{\bar{\tau}}(\bar{f}_\alpha - \bar{f}_\alpha^{eq}) \\ &- Z_r \left[\frac{(2\bar{\tau} - 1)e_{\alpha r}\delta t}{2\bar{\tau} r}\right](\bar{f}_\alpha - \bar{f}_\alpha^{eq}) \\ &+ w_\alpha S_\phi \delta t,\end{aligned} \tag{26}$$

where $\bar{f}_\alpha$ is the distribution function; $\bar{f}_\alpha^{eq}$ is the local equilibrium distribution function; $\bar{\tau}$ is the single relaxation time; and S_ϕ is the source or sink term defined by

$$S_\phi = -\frac{2\rho u_r u_\phi}{r} - \frac{\rho\nu u_\phi}{r^2}. \tag{27}$$

There are many expressions for $\bar{f}_\alpha^{eq}$ and a simple one is used here [15],

$$\bar{f}_\alpha^{eq} = w_\alpha \left(1 + \frac{3 e_{\alpha j} u_j}{e^2}\right)\rho u_\phi. \tag{28}$$

It is easy to show that the above equation has the following properties,

$$\sum_{\alpha} \bar{f}_{\alpha}^{eq} = \rho u_{\phi}, \tag{29}$$

$$\sum_{\alpha} e_{\alpha i} \bar{f}_{\alpha}^{eq} = \rho u_i u_{\phi} \tag{30}$$

and

$$\sum_{\alpha} e_{\alpha i} e_{\alpha j} \bar{f}_{\alpha}^{eq} = \rho e^2 u_{\phi} \delta_{ij}/3. \tag{31}$$

To formulate a macroscopic lattice Boltzmann method for calculating u_{ϕ}, Eq. (26) is rewritten as

$$\begin{aligned} \bar{f}_{\alpha}(\mathbf{x}, t) &= \bar{f}_{\alpha}(\mathbf{x} - \mathbf{e}_{\alpha}\delta t, t - \delta t) - \frac{1}{\bar{\tau}}[(\bar{f}_{\alpha}(\mathbf{x} - \mathbf{e}_{\alpha}\delta t, t - \delta t) \\ &- \bar{f}_{\alpha}^{eq}(\mathbf{x} - \mathbf{e}_{\alpha}\delta t, t - \delta t)] \\ &- Z_r \left[\frac{(2\bar{\tau} - 1) e_{\alpha r} \delta t}{2\bar{\tau} r} \right] \bar{f}_{\alpha}^{neq} + w_{\alpha} S_{\phi} \delta t, \end{aligned} \tag{32}$$

in which $\bar{f}_{\alpha}^{neq}$ is the non-equilibrium distribution function,

$$\bar{f}_{\alpha}^{neq} = \bar{f}_{\alpha} - \bar{f}_{\alpha}^{eq}. \tag{33}$$

Setting $\bar{\tau} = 1$ and taking $\sum$Eq. (32) following Zhou's idea [21] lead to

$$\begin{aligned} \sum \bar{f}_{\alpha}(\mathbf{x}, t) &= \sum \bar{f}_{\alpha}^{eq}(\mathbf{x} - \mathbf{e}_{\alpha}\delta t, t - \delta t)] \\ &- Z_r \frac{\delta t}{2r} \sum e_{\alpha r} \bar{f}_{\alpha}^{neq} + \sum w_{\alpha} S_{\phi} \delta t, \end{aligned} \tag{34}$$

The mass conservation requires $\sum \bar{f}_{\alpha}(\mathbf{x}, t) = \rho u_{\phi}$, i.e., Eq. (34) can be written as

$$\begin{aligned} \rho(\mathbf{x}, t) u_{\phi}(\mathbf{x}, t) &= \sum \bar{f}_{\alpha}^{eq}(\mathbf{x} - \mathbf{e}_{\alpha}\delta t, t - \delta t) \\ &- Z_r \frac{\delta t}{2r} \sum e_{\alpha r} \bar{f}_{\alpha}^{neq} + \sum w_{\alpha} S_{\phi} \delta t, \end{aligned} \tag{35}$$

from which u_{ϕ} is determined after f_{α}^{neq} is estimated using [25]

$$\bar{f}_{\alpha}^{neq}(\mathbf{x}, t) = -[\bar{f}_{\alpha}^{eq}(\mathbf{x}, t) - \bar{f}_{\alpha}^{eq}(\mathbf{x} - \mathbf{e}_{\alpha}\delta t, t - \delta t)]. \tag{36}$$

The centred scheme [24] is again used for term S_{ϕ},

$$S_{\phi} = S_{\phi}\left(\mathbf{x} - \frac{1}{2}\mathbf{e}_{\alpha}\delta t, t - \frac{1}{2}\delta t\right). \tag{37}$$

3.3. Significance

The proposed MacAxLAB has three main distinguishable advantages from existing lattice Boltzmann methods for axisymmetric flows, First of all, only lattice size δx is required to model flows without tuning other calculation parameters such as time step, reducing computational cost. Then, physical variables are directly either retained as Dirichlet boundary condition without additional calculations for boundary lattice points or used as boundary conditions without being converted to particle distribution functions, saving computational time and increasing accuracy due to avoidance of errors from the conversion between the variables and particle distribution functions. Finally, there is no need for computation of particle distribution functions, saving computer storage and accelerating simulation. As such, the developed model is more efficient and accurate.

4. Numerical simulations

4.1. 3D Womersley flow

The 3D Womersley flow or a pulsatile flow is an unsteady axisymmetric flow in a straight pipe. It is driven by a periodic pressure gradient at the inlet of the pipe and the pressure gradient is normally given as

$$\frac{dp}{dx} = p_0 \cos(\omega t), \tag{38}$$

where p_0 is the maximum amplitude of the pressure variation and $\omega = 2\pi/T$ is the angular frequency, in which T is the period. The Reynolds number is defined as $R_e = U_c D/\nu$ with the characteristic velocity U_c given by

$$U_c = \frac{p_0 \alpha^2}{4\omega\rho} = \frac{p_0 R^2}{4\rho\nu}, \tag{39}$$

in which $\alpha = R\sqrt{\omega/\nu}$ is the Womersley number, where R is the pipe radius and D is the diameter. The analytical solution for the velocity component in axial direction is

$$u_x(r,t) = \mathrm{Re}\left\{ \frac{p_0}{i\omega\rho} \left[1 - \frac{J_0(r\phi/R)}{J_0(\phi)} \right] e^{i\omega t} \right\}, \tag{40}$$

where J_0 is the zeroth order Bessel function of the first type; i is the imaginary unit; $\phi = (-\alpha + i\alpha)/\sqrt{2}$; and Re denotes the real part of a complex number.

The implementation of the periodic pressure gradient can be achieved by applying an equivalent periodic body force to the flow [29], i.e., an additional body force is added to the existing force term F_i,

$$F_i = -\frac{\rho u_i u_r}{r} - \frac{2\rho\nu u_i}{r^2}\delta_{ir} + p_0\cos(\omega t)\delta_{ix}. \tag{41}$$

In the computation, $\rho = 3$, $p_0 = 0.001$, $D = 40$, $T = 1200$, $\alpha = 8$, $U_C = 1$, which give $R_e = 1200$. 80×40 lattices with $\Delta x = 1$ are used in the simulation. The periodic boundary conditions are applied to inflow and outflow boundaries; the exact initial zero velocities are retained along the pipe walls for exact no-slip boundary conditions without errors as all computations are carried out on lattice points only within the pipe. The numerical solutions at different times are obtained after initial running time of $10T$. The corresponding results for velocity u_x are shown in Figs. 2 and 3, which are further compared with the analytical solution (40), showing good agreements. Compared to the previously developed AxLAB®, the present MacAxLAB produce more accurate results for $n = 0,\ 1,\ 7,\ 8,\ 9,\ 10,\ 15$ and similarly accurate results for others as shown in Figs. 2 and 3.

4.2. Cylindrical cavity flow

Steady cylindrical cavity flows have been investigated both experimentally and numerically [14, 15, 30, 31]. The flow problem is known to have different complex structures depending on combinations of the aspect ratio $A = H/R$ and the Reynolds number $R_e = R^2\Omega/\nu$, where Ω is the the constant angular velocity; and H is the height of the cylinder. For example, the flow contains a pair of vortex breakdown bubbles when $A = 1.5$ and $R_e = 1290$. Because of its complexity, this case is widely used a benchmark test to validate a numerical method such as the 3D lattice Boltzmann method by Bhaumik and Lakshmisha [31], the axisymmetric lattice Boltzmann method by Guo et al. [14], and the axisymmetric lattice Boltzmann scheme by Li [15]. It is then chosen to test the proposed MacAxLAB. In the simulations, $R = 1$, $\rho = 1$, and $\Omega = 0.1$. The steady flow state is reached after certain time steps when the following convergence criterion is satisfied [14],

$$\frac{\|\mathbf{V}(t) - \mathbf{V}(t - 1000\delta t)\|}{\|\mathbf{V}(t)\|} < 10^{-6}, \tag{42}$$

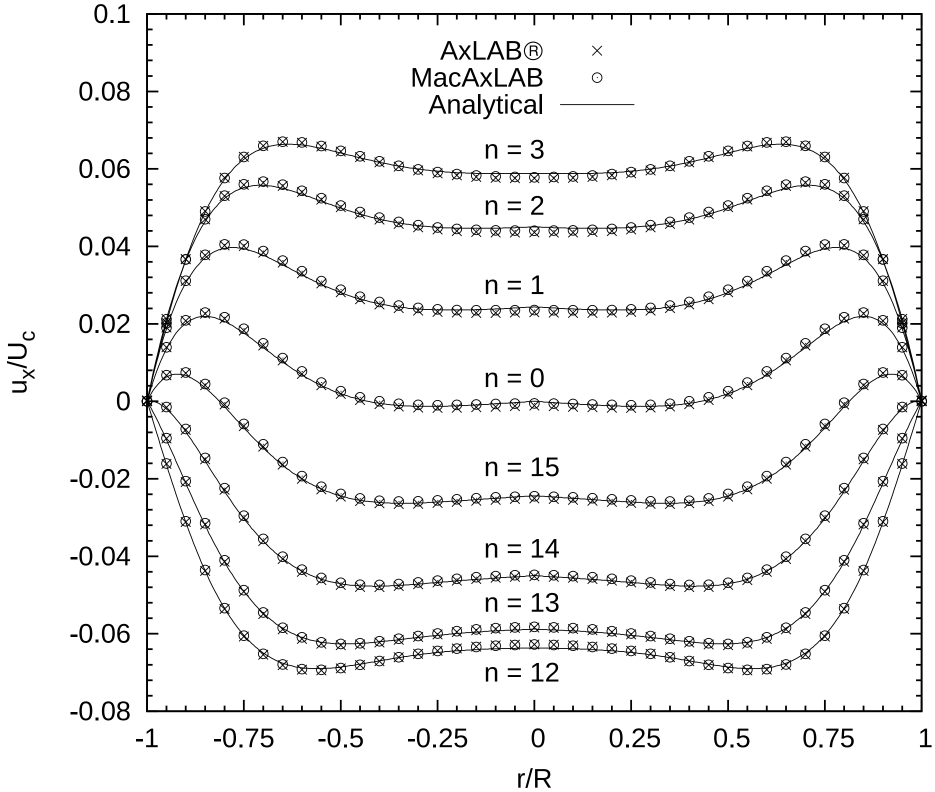

Figure 2: Comparisons of numerical results with analytical solution when u_x is increasing with time at $t = nT/16$ with $n = 0, 1, 2, 3, 12, 13, 14, 15$.

in which $\|\mathbf{V}(t)\| = \sqrt{\sum[u_x^2(x,r) + u_r^2(x,r)]}$. The boundary conditions are

$$\begin{aligned} &u_x = u_r = u_\phi = 0, &&x = 0, \\ &u_x = u_r = u_\phi = 0, &&r = \pm R, \\ &u_x = u_r = 0, u_\phi = r\Omega, &&x = H, \end{aligned} \tag{43}$$

which are directly determined once and retained as boundary conditions in the proposed model as calculations are required only within the cylinder during simulation. This avoid the additional errors induced by using other scheme such as bounce back or nonequilibrium extrapolation approach [32]. The streamlines for the steady solution are plotted in Fig. 4 and clearly show that a pair of vortex breakdown bubbles is well developed. This is again in agreement with that observed in the experimental measurements

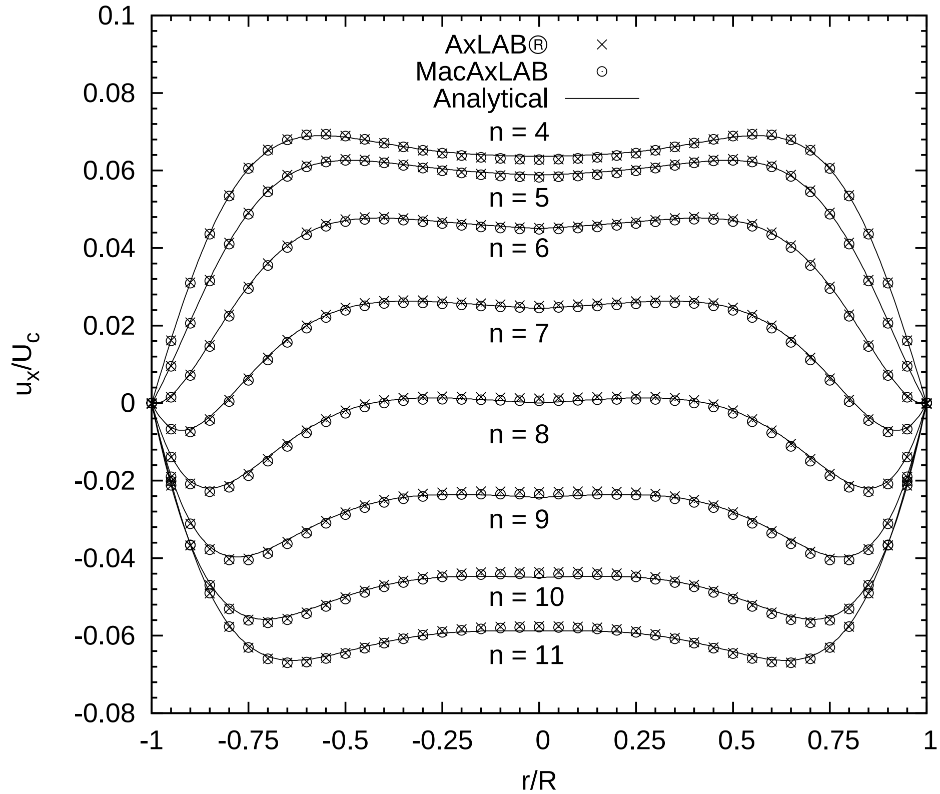

Figure 3: Comparisons of numerical results with analytical solution when u_x is decreasing with time at $t = nT/16$ with $n = 4, 5, 6, 7, 8, 9, 10, 11$.

[30] and the numerical results [14, 15, 20, 31]. The maximum axial velocity $u_{x,max}$ and its location h_{max} are shown in Table 1 and further compared with the existing experimental data and other numerical results from the AxLAB®, the improved model by by Li et al. [15], the 3D LBM and the Navier-Stokes solutions by Bhaumik and Lakshmisha [31]. The relative errors calculated for velocity using $E_u = (u_{x,max} - u'_{x,max})/u'_{x,max}$, and for location using $E_u = (h_{max} - h'_{max})/h'_{max}$, where $u_{x,max}$ stands for numerical result, $u'_{x,max}$ for experimental data, h_{max} and h'_{max} are the locations from computation and measurement in laboratory, respectively. As seen from Table 1, $E_u = 4.71\%$ and $E_h = 5\%$ are among Li's model, the 3D LBM solution and the Navier-Stokes result. This again indicates that the present model can produce accurate solutions, agreeing well with the previous investigations.

Table 1: Comparisons of maximum axial velocities.

Model	$u_{x,max}/u_0$	h_{max}/H	E_u	E_h
MacAxLAB	0.0712	0.147	4.71%	5.00%
AxLAB® [20]	0.0706	0.147	3.82%	5.00%
3D LBM [31]	0.072	0.16	5.88%	14.29%
N-S [31]	0.0665	0.125	2.21%	5.0%
Li's LBM [15]	0.0716	0.147	5.29%	5.00%
Expt. [30]	0.068	0.14	–	–

Note: $R = 1$, $\Omega = 0.1$ and $u_0 = R\Omega$.

To demonstrate the potential of the present method in predicting more complex axisymmetric flow, a further case with $A = 2.5$ and $R_e = 2200$ is simulated. This case has also been investigated in the experiment [30], revealing that there are two vortex breakdown bubbles. The other calculating parameters remain the same as those in the first case. The stream lines for the steady solution are plotted in Fig. 5 and clearly show that two pairs of vortex breakdown bubbles are well developed. The flow pattern is again in agreement with that observed in the experimental measurements [30].

5. Conclusions

A macroscopic axisymmetric lattice Boltzmann method (MacAxLAB) is described for generic axisymmetric flows with or without swirling. No collision operator is involved and the scheme is unconditionally stable. The main features are (i) the Dirichlet boundary condition can exactly be achieved without using other scheme such as bounce-back scheme, the macroscopic variable are directly used for other boundary conditions without recourse to particle distribution functions; (ii) it requires less memory in simulations; and (iii) there is no calculation for data transfer between particle distributions and macroscopic variables. Three numerical examples have shown that the MacAxLAB is simple and accurate, which is suitable for both steady and unsteady axisymmetric rotational flows.

Appendix A Recovery of the Axisymmetric Flow Equations

In order to recover the axisymmetric flow equations from the MacAxLAB, we take a Taylor expansion to the terms on the right-hand side of Eq. (13),

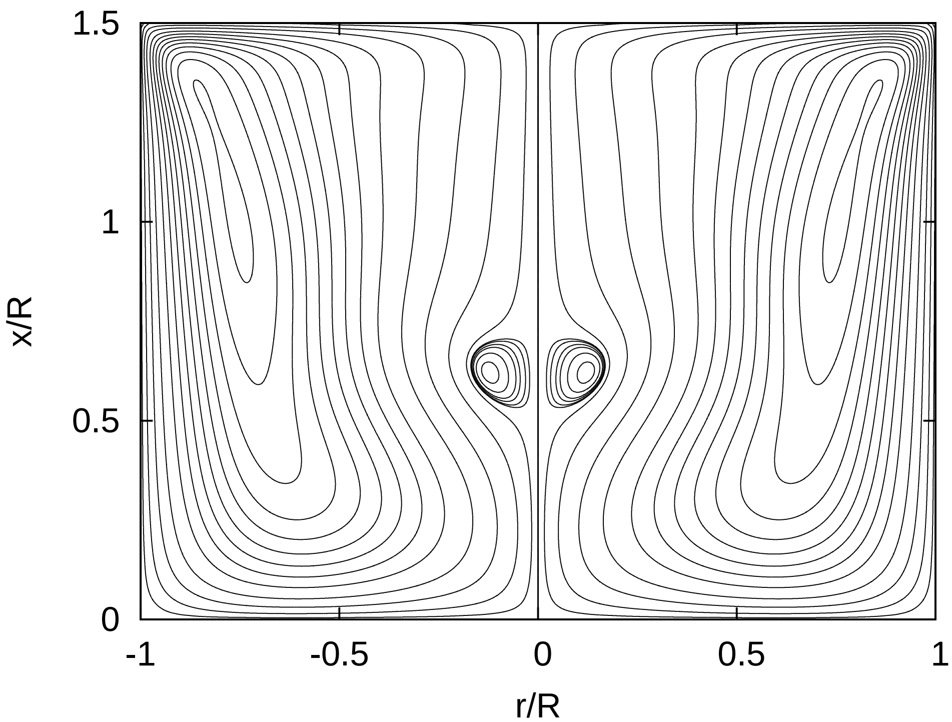

Figure 4: Streamlines for the case with $A = 1.5$ and $R_e = 1290$, showing a pair of the fully developed vortex breakdown bubbles.

$f_\alpha(\mathbf{x}-\mathbf{e}_\alpha\delta t, t-\delta t)$ and $f_\alpha^{eq}(\mathbf{x}-\mathbf{e}_\alpha\delta t, t-\delta t)$, in time and space at point $(\mathbf{x}, t)$, and have

$$\begin{aligned} f_\alpha(\mathbf{x}-\mathbf{e}_\alpha\delta t, t-\delta t) &= f_\alpha - \delta t\left(\frac{\partial}{\partial t} + e_{\alpha j}\frac{\partial}{\partial x_j}\right) f_\alpha \\ &+ \frac{1}{2}\delta t^2\left(\frac{\partial}{\partial t} + e_{\alpha j}\frac{\partial}{\partial x_j}\right)^2 f_\alpha + \mathcal{O}(\delta t^3) \qquad \text{(A.1)} \end{aligned}$$

and

$$f_\alpha^{eq}(\mathbf{x}-\mathbf{e}_\alpha\delta t, t-\delta t) = f_\alpha^{eq} - \delta t\left(\frac{\partial}{\partial t} + e_{\alpha j}\frac{\partial}{\partial x_j}\right) f_\alpha^{eq}$$

$$+ \quad \frac{1}{2}\delta t^2 \left(\frac{\partial}{\partial t} + e_{\alpha j} \frac{\partial}{\partial x_j} \right)^2 f_\alpha^{eq} + \mathcal{O}(\delta t^3). \quad \text{(A.2)}$$

According to the Chapman-Enskog analysis, f_α can be expanded in a series of δt,

$$f_\alpha = f_\alpha^{(0)} + \delta t f_\alpha^{(1)} + \delta t^2 f_\alpha^{(2)} + \mathcal{O}(\delta t^3). \quad \text{(A.3)}$$

Eqs. (20) and (21) can also be written, via a Taylor expansion, as

$$\theta \left(\mathbf{x} - \frac{1}{2}\mathbf{e}_\alpha \delta t, t - \frac{1}{2}\delta t \right) = \theta - \frac{\delta t}{2} \left(\frac{\partial}{\partial t} + e_{\alpha j} \frac{\partial}{\partial x_j} \right) \theta + \mathcal{O}(\delta t^2) \quad \text{(A.4)}$$

and

$$F_i \left(\mathbf{x} - \frac{1}{2}\mathbf{e}_\alpha \delta t, t - \frac{1}{2}\delta t \right) = F_i - \frac{\delta t}{2} \left(\frac{\partial}{\partial t} + e_{\alpha j} \frac{\partial}{\partial x_j} \right) F_i + \mathcal{O}(\delta t^2) \quad \text{(A.5)}$$

After substitution of Eqs. (A.1) - (A.5) into Eq. (13), we have the expressions to order δt^0

$$f_\alpha^{(0)} = f_\alpha^{eq}, \quad \text{(A.6)}$$

to order δt

$$\left(\frac{\partial}{\partial t} + e_{\alpha j} \frac{\partial}{\partial x_j} \right) f_\alpha^{(0)} = -\frac{f_\alpha^{(1)}}{\tau} + w_\alpha \theta + 3 w_\alpha \frac{e_{\alpha i}}{e^2} F_i, \quad \text{(A.7)}$$

and to order δt^2

$$\begin{aligned} \left(\frac{\partial}{\partial t} + e_{\alpha j} \frac{\partial}{\partial x_j} \right) f_\alpha^{(1)} - \frac{1}{2} \left(\frac{\partial}{\partial t} + e_{\alpha j} \frac{\partial}{\partial x_j} \right)^2 f_\alpha^{(0)} &= -\frac{f_\alpha^{(2)}}{\tau} \\ + \frac{1}{\tau} \left(\frac{\partial}{\partial t} + e_{\alpha j} \frac{\partial}{\partial x_j} \right) f_\alpha^{(1)} - \frac{(2\tau - 1)}{2\tau r} e_{\alpha r} f_\alpha^{(1)} & \\ - \frac{w_\alpha}{2} \left(\frac{\partial}{\partial t} + e_{\alpha j} \frac{\partial}{\partial x_j} \right) \theta - \frac{3 w_\alpha e_{\alpha i}}{2e^2} \left(\frac{\partial}{\partial t} + e_{\alpha j} \frac{\partial}{\partial x_j} \right) F_i. & \quad \text{(A.8)} \end{aligned}$$

Using Eq. (A.7), we can write the above equation as

$$\frac{(2\tau - 1)}{2\tau} \left(\frac{\partial}{\partial t} + e_{\alpha j} \frac{\partial}{\partial x_j} \right) f_\alpha^{(1)} = -\frac{f_\alpha^{(2)}}{\tau} - \frac{(2\tau - 1)}{2\tau r} e_{\alpha r} f_\alpha^{(1)}. \quad \text{(A.9)}$$

From Eq. (A.7) + Eq. (A.9) $\times\delta t$, we have

$$\left(\frac{\partial}{\partial t}+e_{\alpha j}\frac{\partial}{\partial x_j}\right)f_\alpha^{(0)}+\frac{(2\tau-1)\delta t}{2\tau}\left(\frac{\partial}{\partial t}+e_{\alpha j}\frac{\partial}{\partial x_j}\right)f_\alpha^{(1)}$$
$$=-\frac{1}{\tau}(f_\alpha^{(1)}+\delta t f_\alpha^{(2)})-\frac{(2\tau-1)\delta t}{2\tau r}e_{\alpha r}f_\alpha^{(1)}$$
$$+w_\alpha\theta+\frac{3w_\alpha}{e^2}e_{\alpha i}F_i. \tag{A.10}$$

Summation of the above equation over α provides

$$\frac{\partial}{\partial t}\sum_\alpha f_\alpha^{(0)}+\frac{\partial}{\partial x_j}\sum_\alpha e_{\alpha j}f_\alpha^{(0)}=\theta. \tag{A.11}$$

Using Eq. (A.6) and substitution of Eq. (12) into the above equation result in the continuity equation (1), if the density variation is small enough and can be neglected.

Taking $\sum e_{\alpha i}[$ (A.7) + $\delta t\times$ (A.9)] about α yields

$$\frac{\partial}{\partial t}\sum_\alpha e_{\alpha i}f_\alpha^{(0)}+\frac{\partial \Pi_{ij}^{(0)}}{\partial x_j}=\frac{\partial\Lambda_{ij}}{\partial x_j}+\frac{\Lambda_{ir}}{r}+F_i, \tag{A.12}$$

where $\Pi_{ij}^{(0)}$ is the zeroth-order momentum flux tensor given by the following expression,

$$\Pi_{ij}^{(0)}=\sum_\alpha e_{\alpha i}e_{\alpha j}f_\alpha^{(0)}, \tag{A.13}$$

$$\Lambda_{ij}=-\frac{\delta t}{2\tau}(2\tau-1)\sum_\alpha e_{\alpha i}e_{\alpha j}f_\alpha^{(1)}, \tag{A.14}$$

and

$$\Lambda_{ir}=-\frac{\delta t}{2\tau}(2\tau-1)\sum_\alpha e_{\alpha i}e_{\alpha r}f_\alpha^{(1)}. \tag{A.15}$$

Evaluating terms in Eq. (A.13) with Eq. (11), we have

$$\Pi_{ij}^{(0)}=p\delta_{ij}+\rho u_i u_j, \tag{A.16}$$

where $p=\rho e^2/3$ is the pressure, leading to a sound speed, $C_s=e/\sqrt{3}$. Substitution of the above equation into Eq. (A.12) produces

$$\frac{\partial(\rho u_i)}{\partial t}+\frac{\partial(\rho u_i u_j)}{\partial x_j}=-\frac{\partial p}{\partial x_i}+\frac{\partial\Lambda_{ij}}{\partial x_j}+\frac{\Lambda_{ir}}{r}+F_i. \tag{A.17}$$

Applying Eq. (A.7), we can rewrite Eq. (A.14) as

$$\Lambda_{ij} = \Pi_{ij}^{(1)} - \frac{\delta t}{2}(2\tau - 1)\sum_{\alpha} e_{\alpha i}e_{\alpha j}w_\alpha \theta, \tag{A.18}$$

with the first-order momentum flux tensor $\Pi_{ij}^{(1)}$ defined by,

$$\Pi_{ij}^{(1)} = \frac{\delta t}{2}(2\tau - 1)\sum_{\alpha} e_{\alpha i}e_{\alpha j}\left(\frac{\partial}{\partial t} + e_{\alpha k}\frac{\partial}{\partial x_k}\right) f_\alpha^{(0)}, \tag{A.19}$$

which can also be written using Eq. (A.13) as,

$$\Pi_{ij}^{(1)} = \frac{\delta t}{2}(2\tau - 1)\frac{\partial}{\partial t}\Pi_{ij}^{(0)} + \frac{\delta t}{2}(2\tau - 1)\frac{\partial}{\partial x_k}\sum_{\alpha} e_{\alpha i}e_{\alpha j}e_{\alpha k} f_\alpha^{(0)}. \tag{A.20}$$

The second term in the above equation can be evaluated with Eq. (11) and Eq. (A.6) as

$$\frac{\partial}{\partial x_k}\sum_{\alpha} e_{\alpha i}e_{\alpha j}e_{\alpha k} f_\alpha^{(0)} = \frac{e^2}{3}\frac{\partial}{\partial x_k}(\rho u_i \delta_{jk} + \rho u_j \delta_{ki} + \rho u_k \delta_{ij}). \tag{A.21}$$

If we assume that characteristic velocity is U_c, length L_c and time t_c, we have that the term $(\partial/\partial t \Pi_{ij}^{(0)})$ is of order $\rho U_c^2/t_c$ and the term $(\partial/\partial x_k \sum_\alpha e_{\alpha i}e_{\alpha j}e_{\alpha k} f_\alpha^{(0)})$ is of order $\rho e^2 U_c/L_c$, based on which we obtain that the ratio of the former to the latter terms has the order,

$$\begin{aligned}\mathcal{O}\left(\frac{\partial/\partial t \Pi_{ij}^{(0)}}{\partial/\partial x_k \sum_\alpha e_{\alpha i}e_{\alpha j}e_{\alpha k} f_\alpha^{(0)}}\right) &= \mathcal{O}\left(\frac{\rho U_c^2/t_c}{\rho e^2 U_c/L_c}\right) \\ &= \mathcal{O}\left(\frac{U_c}{e}\right)^2 = \mathcal{O}\left(\frac{U_c}{C_s}\right)^2 = \mathcal{O}(M^2),\end{aligned} \tag{A.22}$$

in which $M = U_c/C_s$ is the Mach number. It follows that the first term in Eq. (A.20) is very small compared with the second term and can be neglected if $M << 1$ which is consistent with the lattice Boltzmann dynamics; hence Eq. (A.20), after Eq. (A.21) is substituted, becomes

$$\Pi_{ij}^{(1)} = \frac{e^2\delta t}{6}(2\tau - 1)\frac{\partial}{\partial x_k}(\rho u_i \delta_{jk} + \rho u_j \delta_{ki} + \rho u_k \delta_{ij}), \tag{A.23}$$

or

$$\Pi_{ij}^{(1)} = \nu \left[\frac{\partial(\rho u_i)}{\partial x_j} + \frac{\partial(\rho u_j)}{\partial x_i} + \frac{\partial(\rho u_k)}{\partial x_k}\delta_{ij} \right], \tag{A.24}$$

where ν is the kinematic viscosity and defined by

$$\nu = \frac{e^2 \delta t}{6}(2\tau - 1). \tag{A.25}$$

Inserting (A.24) into Eq. (A.18) and evaluating the rest terms of the equation lead to

$$\Lambda_{ij} = \nu \left[\frac{\partial(\rho u_i)}{\partial x_j} + \frac{\partial(\rho u_j)}{\partial x_i} + \frac{\partial(\rho u_k)}{\partial x_k}\delta_{ij} \right] - \nu\theta\delta_{ij}. \tag{A.26}$$

After applying the continuity equation (1) and Eq. (5) to the above, we obtain

$$\Lambda_{ij} = \nu \left[\frac{\partial(\rho u_i)}{\partial x_j} + \frac{\partial(\rho u_j)}{\partial x_i} \right]. \tag{A.27}$$

Similarly, we have

$$\Lambda_{ir} = \nu \left[\frac{\partial(\rho u_i)}{\partial r} + \frac{\partial(\rho u_r)}{\partial x_i} \right]. \tag{A.28}$$

Combining Eqs. (6), (A.27) and (A.28) with Eq. (A.17) results in

$$\begin{aligned} \frac{\partial(\rho u_i)}{\partial t} &+ \frac{\partial(\rho u_i u_j)}{\partial x_j} = -\frac{\partial p}{\partial x_i} + \nu \frac{\partial}{\partial x_j}\left[\frac{\partial(\rho u_i)}{\partial x_j} + \frac{\partial(\rho u_j)}{\partial x_i} \right] \\ &+ \frac{\nu}{r}\left[\frac{\partial(\rho u_i)}{\partial r} + \frac{\partial(\rho u_r)}{\partial x_i} \right] - \frac{\rho u_i u_r}{r} - \frac{2\rho\nu u_i}{r^2}\delta_{ir}. \end{aligned} \tag{A.29}$$

Again, if the density variation is assumed to be small enough, the above is just the momentum equation (2). As τ takes a constant, use of $\tau = 1$ also recovers the continuity and the axisymmetric flow equations at the second-order accurate as the above derivation shows. In this case, Eq. (A.25) becomes Eq. (23), which determines the particle speed e.

Appendix B Recovery of the equation for azimuthal velocity

In order to prove that Eq. (24) can be recovered from the lattice Boltzmann equation (32), we apply the similar Chapman-Enskog analysis to that given in Appendix A and, after taking a Taylor expansion to $\bar{f}_\alpha(\mathbf{x} - \mathbf{e}_\alpha \delta t, t -$

$\delta t)$ and $\bar{f}_\alpha^{eq}(\mathbf{x} - \mathbf{e}_\alpha \delta t, t - \delta t)$ on the right-hand side of Eq. (32) in time and space at point $(\mathbf{x}, t)$, we have

$$\begin{aligned} \bar{f}_\alpha(\mathbf{x} - \mathbf{e}_\alpha \delta t, t - \delta t) &= \bar{f}_\alpha - \delta t \left(\frac{\partial}{\partial t} + e_{\alpha j} \frac{\partial}{\partial x_j} \right) \bar{f}_\alpha \\ &+ \frac{1}{2} \delta t^2 \left(\frac{\partial}{\partial t} + e_{\alpha j} \frac{\partial}{\partial x_j} \right)^2 \bar{f}_\alpha + \mathcal{O}(\delta t^3), \end{aligned} \tag{B.1}$$

$$\begin{aligned} \bar{f}_\alpha^{eq}(\mathbf{x} - \mathbf{e}_\alpha \delta t, t - \delta t) &= \bar{f}_\alpha^{eq} - \delta t \left(\frac{\partial}{\partial t} + e_{\alpha j} \frac{\partial}{\partial x_j} \right) \bar{f}_\alpha^{eq} \\ &+ \frac{1}{2} \delta t^2 \left(\frac{\partial}{\partial t} + e_{\alpha j} \frac{\partial}{\partial x_j} \right)^2 \bar{f}_\alpha^{eq} + \mathcal{O}(\delta t^3). \end{aligned} \tag{B.2}$$

Eq. (37) is also written, via a Taylor expansion, as

$$\begin{aligned} S_\phi \left(\mathbf{x} - \frac{1}{2} \mathbf{e}_\alpha \delta t, t - \frac{1}{2} \delta t \right) &= S_\phi(\mathbf{x}, t) \\ &- \frac{1}{2} \delta t \left(\frac{\partial}{\partial t} + e_{\alpha i} \frac{\partial}{\partial x_i} \right) S_\phi(\mathbf{x}, t) + \mathcal{O}(\delta t^2). \end{aligned} \tag{B.3}$$

From the Chapman-Enskog expansion, we have

$$\bar{f}_\alpha = \bar{f}_\alpha^{(0)} + \delta t \bar{f}_\alpha^{(1)} + \delta t^2 \bar{f}_\alpha^{(2)} + \mathcal{O}(\delta t^3). \tag{B.4}$$

After substitution of Eqs. (B.1), (B.2), (B.3) and (B.4) into Eq. (32), the equation is to order δt^0

$$\bar{f}_\alpha^{(0)} = \bar{f}_\alpha^{eq}, \tag{B.5}$$

to order δt

$$\left(\frac{\partial}{\partial t} + e_{\alpha j} \frac{\partial}{\partial x_j} \right) \bar{f}_\alpha^{(0)} = - \frac{\bar{f}_\alpha^{(1)}}{\tau} + w_\alpha S_\phi, \tag{B.6}$$

and to order δt^2

$$\begin{aligned} \left(\frac{\partial}{\partial t} + e_{\alpha j} \frac{\partial}{\partial x_j} \right) \bar{f}_\alpha^{(1)} - \frac{1}{2} \left(\frac{\partial}{\partial t} + e_{\alpha j} \frac{\partial}{\partial x_j} \right)^2 \bar{f}_\alpha^{(0)} &= - \frac{\bar{f}_\alpha^{(2)}}{\tau} \\ + \frac{1}{\tau} \left(\frac{\partial}{\partial t} + e_{\alpha j} \frac{\partial}{\partial x_j} \right) \bar{f}_\alpha^{(1)} - \frac{(2\tau - 1)}{2\tau r} e_{\alpha r} \bar{f}_\alpha^{(1)} & \\ - \frac{w_\alpha}{2} \left(\frac{\partial}{\partial t} + e_{\alpha i} \frac{\partial}{\partial x_i} \right) S_\phi. & \end{aligned} \tag{B.7}$$

Substitution of Eq. (B.6) into the above equation gives

$$\frac{(2\tau-1)}{2\tau}\left(\frac{\partial}{\partial t}+e_{\alpha i}\frac{\partial}{\partial x_i}\right)\bar{f}_\alpha^{(1)}=-\frac{\bar{f}_\alpha^{(2)}}{\tau}-\frac{(2\tau-1)}{2\tau r}e_{\alpha r}\bar{f}_\alpha^{(1)}. \tag{B.8}$$

Taking $\sum$ [Eq. (B.6) + $\delta t\times$ Eq. (B.8)] yields

$$\frac{\partial}{\partial t}\sum_\alpha \bar{f}_\alpha^{(0)}+\frac{\partial}{\partial x_i}\sum_\alpha e_{\alpha i}\bar{f}_\alpha^{(0)}=\frac{\partial \Gamma_i}{\partial x_i}+\frac{\Gamma_r}{r}+S_\phi, \tag{B.9}$$

where

$$\Gamma_i=-\frac{(2\tau-1)\delta t}{2\tau}\sum_\alpha e_{\alpha i}\bar{f}_\alpha^{(1)}, \tag{B.10}$$

and

$$\Gamma_r=-\frac{(2\tau-1)\delta t}{2\tau}\sum_\alpha e_{\alpha r}\bar{f}_\alpha^{(1)}. \tag{B.11}$$

Inserting Eq. (B.6) into Eq. (B.10) leads to

$$\Gamma_i=\frac{\delta t}{2}(2\tau-1)\sum_\alpha e_{\alpha i}\left(\frac{\partial}{\partial t}+e_{\alpha j}\frac{\partial}{\partial x_j}\right)\bar{f}_\alpha^{(0)}, \tag{B.12}$$

or

$$\Gamma_i=\frac{\delta t}{2}(2\tau-1)\left(\frac{\partial}{\partial t}\sum_\alpha e_{\alpha i}\bar{f}_\alpha^{(0)}+\frac{\partial}{\partial x_j}\sum_\alpha e_{\alpha i}e_{\alpha j}\bar{f}_\alpha^{(0)}\right). \tag{B.13}$$

The order analysis indicates that $\partial/\partial t\sum_\alpha e_{\alpha i}\bar{f}_\alpha^{(0)}$ has order of $\rho U_c^2/t_c$ from Eq. (30), and $\partial/\partial x_j\sum_\alpha e_{\alpha i}e_{\alpha j}\bar{f}_\alpha^{(0)}$ has order of $\rho e^2 U_c/L_c$ from Eq. (31), based on which the ratio of the former to the latter has the order of

$$\begin{aligned}\mathcal{O}\left(\frac{\partial/\partial t\sum_\alpha e_{\alpha i}\bar{f}_\alpha^{(0)}}{\partial/\partial x_j\sum_\alpha e_{\alpha i}e_{\alpha j}\bar{f}_\alpha^{(0)}}\right)&=\mathcal{O}\left(\frac{\rho U_c^2/t_c}{\rho e^2 U_c/L_c}\right)\\&=\mathcal{O}\left(\frac{U_c}{e}\right)^2=\mathcal{O}\left(\frac{U_c}{C_s}\right)^2=\mathcal{O}(M^2).\end{aligned} \tag{B.14}$$

This suggests that the first term in Eq. (B.13) is much smaller compared to the second and can be dropped if $M << 1$, which again conform to the lattice Boltzmann method; hence Eq. (B.13) can be approximated by

$$\Gamma_i=\frac{\delta t}{2}(2\tau-1)\frac{\partial}{\partial x_j}\sum_\alpha e_{\alpha i}e_{\alpha j}\bar{f}_\alpha^{(0)}. \tag{B.15}$$

Applying Eq. (31) into above, we have

$$\Gamma_i = \nu \frac{\partial(\rho u_\phi)}{\partial x_i}. \tag{B.16}$$

Similarly, we have

$$\Gamma_r = \nu \frac{\partial(\rho u_\phi)}{\partial r}. \tag{B.17}$$

Substitution of Eqs. (29), (30), (B.16) and (B.17) into Eq. (B.9) results in the governing equation (24) if the density variation is assumed to be small enough.

References

[1] M. R. Swift, W. R. Osborn, J. M. Yeomans, Lattice Boltzmann simulation of nonideal fluids, Physical Review Letters 75 (1995) 830–833.

[2] M. A. A. Spaid, F. R. Phelan, Jr., Lattice boltzmann method for modeling microscale flow in fibrous porous media, Phys. Fluids 9 (9) (1997) 2468–2474.

[3] J. G. Zhou, A lattice Boltzmann model for the shallow water equations, Computer methods in Applied Mechanics and Engineering 191 (32) (2002) 3527–3539.

[4] J. G. Zhou, A lattice Boltzmann model for groundwater flows, International Journal of Modern Physics C 18 (2007) 973–991.

[5] Y. Peng, C. Shu, Y. Chew, J. Qiu, Numerical investigation of flows in czochralski crystal growth by an axisymmetric lattice boltzmann method, Journal of Computational Physics 186 (2003) 295–307.

[6] X. D. Niu, C. Shu, Y. T. Chew, An axisymmetric lattice Boltzmann model for simulation of taylor couette flows between two concentric cylinders, International Journal of Modern Physics C 6 (2003) 785–796.

[7] K. N. Premnath, J. Abraham, Lattice Boltzmann model for axisymmetric multiphase flows, Physical Review E 71 (2005) 056706.

[8] T. Reis, T. N. Phillips, Modified lattice Boltzmann model for axisymmetric flows, Physical Review E 75 (2007) 056703.

[9] S. Mukherjee, J. Abraham, Lattice Boltzmann simulations of two-phase flow with high density ratio in axally symmetric geometry, Physical Review E 75 (2007) 026701.

[10] I. Halliday, L. A. Hammond, C. M. Care, K. Good, A. Stevens, Lattice Boltzmann equation hydrodynamics, Physical Review E 64 (2001) 011208.

[11] T. S. Lee, H. Huang, C. Shu, An axisymmetric incompressible lattice BGK model for simulation of the pulsatile flow in a circular pipe, International Journal for Numerical Methods in Fluids 49 (2005) 99–116.

[12] T. S. Lee, H. Huang, C. Shu, An axisymmetric incompressible lattice Boltzmann model for pipe flow, International Journal of Modern Physics C 17 (2006) 645–661.

[13] T. Reis, T. N. Phillips, Erratum: Modified lattice Boltzmann model for axisymmetric flows [phys. rev. e 75, 056703 (2007)], Physical Review E 76 (2007) 059902(E).

[14] Z. Guo, H. Han, B. Shi, C. Zheng, Theory of the lattice Boltzmann equation: Lattice boltzmann model for axisymmetric flows, Physical Review E 79 (2009) 046708.

[15] Q. Li, Y. L. He, G. H. Tang, W. Q. Tao, Improved axisymmetric lattice Boltzmann scheme, Physical Review E 81 (2010) 056707.

[16] J. G. Zhou, Axisymmetric lattice Boltzmann method, Physical Review E 78 (2008) 036701.

[17] H. B. Huang, X. Y. Lu, Theoretical and numerical study of axisymmetric lattice Boltzmann models, Physical Review E 80 (2009) 016701.

[18] X. F. Li, G. H. Tang, T. Y. Gao, W. Q. Tao, Simulation of Newtonian and non-Newtonian axisymmetric flow with an axisymmetric lattice Boltzmann model, International Journal of Modern Physics C 21 (10) (2010) 1237–1254.

[19] G. H. Tang, X. F. Li, W. Q. Tao, Microannular electro-osmotic flow with the axisymmetric lattice boltzmann method, Journal of Applied Physics 108 (11) (2010) 114903.

[20] J. G. Zhou, Axisymmetric lattice Boltzmann method revised, Phys. Rev. E 84 (2011) 036704.

[21] J. G. Zhou, Macroscopic lattice Boltzmann method, arXiv:1901.02716v1.

[22] W. P. Graebel, Engineering Fluid Mechanics, The International Student Edition, Taylor & Francis, London, 2001.

[23] T. Reis, T. N. Phillips, Numerical validation of a consistent axisymmetric lattice Boltzmann model, Physical Review E 77 (2008) 026703.

[24] J. G. Zhou, Lattice Boltzmann Methods for Shallow Water Flows, Springer-Verlag, Berlin, 2004.

[25] C. Shu, Y. Wang, C. J. Teo, J. Wu, Development of lattice Boltzmann flux solver for simulation of incompressible flows, Advances in Applied Mathematics and Mechanics 6 (2014) 436–460.

[26] S. P. Dawson, S. Chen, G. D. Doolen, Lattice boltzmann computations for reaction-diffusion equations, Journal of Chemical Physics 98 (1993) 1514–1523.

[27] S. Chen, J. Tölke, S. Geller, M. Krafczyk, Lattice Boltzmann model for incompressible axisymmetric flows, Physical Review E 78 (2008) 046703.

[28] J. G. Zhou, A lattice Boltzmann method for solute transport, International Journal for Numerical Methods in Fluids 61 (2009) 848–863.

[29] J. A. Cosgrove, J. M. Buick, S. J. Tonge, Application of the lattice Boltzmann method to transition of oscillatory channel flow, Journal of Physics A: Mathematical and General 36 (2003) 2609–2620.

[30] K. Fujimura, H. Yoshizawa, R. Iwatsu, H. Koyama, Velocity measurements of vortex breakdown in an enclosed cylinder, Journal of Fluids Engineering 123 (2001) 604–611.

[31] S. Bhaumik, K. Lakshmisha, Lattice Boltzmann simulation of lid-driven swirling flow in confined cylindrical cavity, Computers and Fluids 36 (2007) 1163–1173.

[32] Z. Guo, C. Zheng, B. Shi, An extrapolation method for boundary conditions in lattice boltzmann method, Physics of Fluids 14 (6) (2002) 2007–2010.

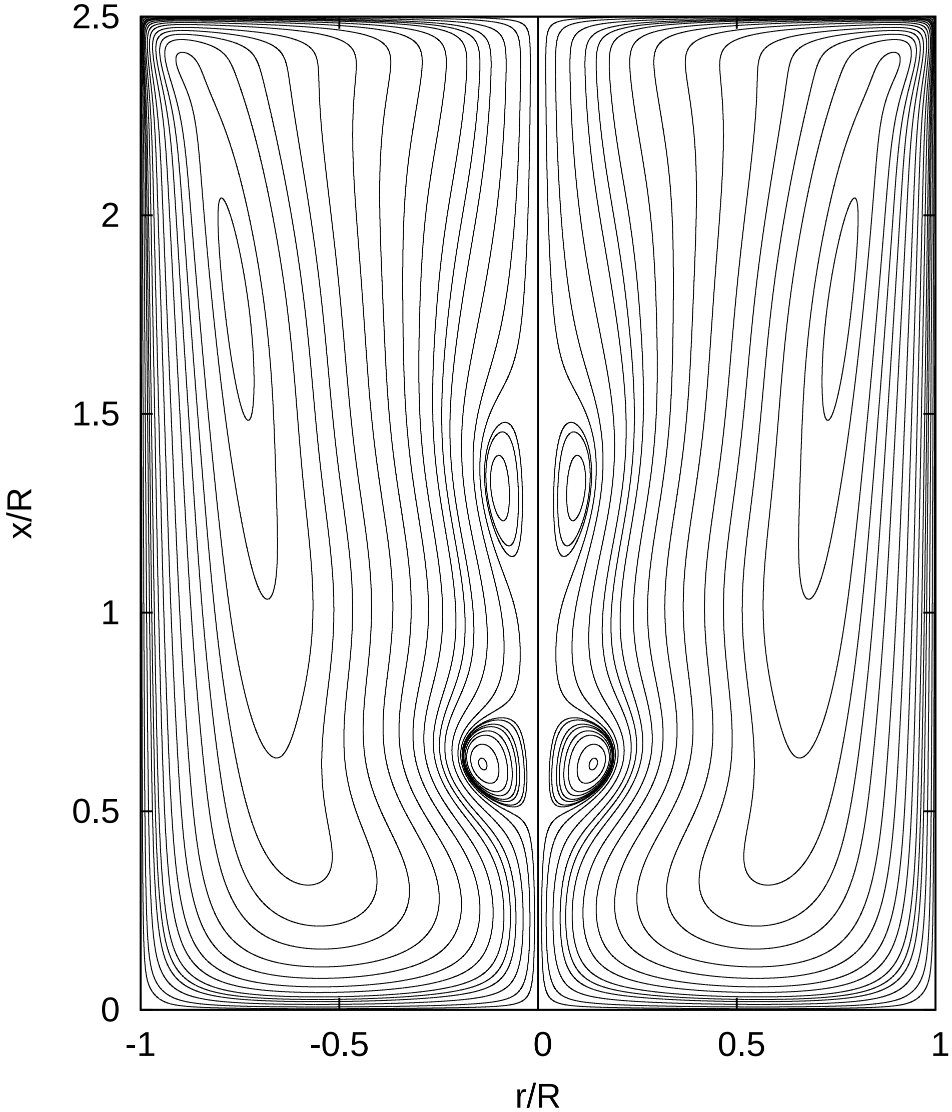

Figure 5: Streamlines for the case with $A = 2.5$ and $R_e = 2200$, showing two pairs of the fully developed vortex breakdown bubbles.